COVID-19 X-ray Image Classification

Maneesh Kumar Singh
University of Illinois at Urbana-Champaign
mksingh4@illinois.edu

Raman Walwyn-Venugopal
University of Illinois at Urbana-Champaign
rsw2@illinois.edu

Satish Reddy Asi
University of Illinois at Urbana-Champaign
sasi2@illinois.edu

Srikanth Bharadwaz Samudrala
University of Illinois at Urbana-Champaign
sbs7@illinois.edu

ABSTRACT

Objective: Detecting COVID-19 using Chest X-Ray (CXR) images is becoming increasingly popular in deep learning research. When training deep neural networks, large and balanced datasets are preferred. However, since COVID-19 is new, there are a limited number of CXR images available which results in a challenge for training deep neural networks. Existing research has shown different approaches to address this imbalanced data issue. Two notable studies are FLANNEL (Focal Loss bAsed Neural Network EnsembLe) model and a patch-based classifier that works on segmented versions of the lung contours. We propose merging these two concepts together to improve performance of detecting COVID-19 in CXR images.

Materials and Methods: Using segmentation networks to create masks for the lungs as a pre-processing step. Replace base models in FLANNEL with patch-based classifiers that take the image and respective mask as their input. The patch-based classifiers will be used as the ensemble.

Results: We are able to reproduce FLANNEL with updated datasets. We created a segmentation network that can produce masks of the lung contours for CXR images and successfully used it to generate masked CXR images of the updated FLANNEL datasets.The FLANNEL base models were successfully to be patch-based classifiers. The overall modifications resulted in similar performance of the original FLANNEL architecture, where some areas improved while others decreased.

Discussion: We saw improvement in metrics when training the base models and FLANNEL ensemble in detecting COVID-19 images. Since no parameters were changed, we suspect that this is due to the large increase of COVID-19 images for the dataset in comparison to when the FLANNEL paper was written. When training the patch-based models, we noticed that some patch-based models slightly improved in performance while others slightly decreased but there were no major differences.

Conclusion: With the Patched FLANNEL barely outperforming FLANNEL in certain metrics, we believe there is merit to conduct further research to determine if more improvements can be made. Potential areas that can be further developed are but not limited to; segmentation, data augmentation, changing number of patches, changing size of patch and more. However, it should be noted that the largest improvement in overall metrics when compared to the original FLANNEL with the old dataset is due to the updated dataset having a large increase in Covid-19 images. This highlights how crucial getting quality data is to improve performance on models.

1. INTRODUCTION

Coronavirus disease 2019 (COVID-19) is a contagious disease caused by severe acute respiratory syndrome Coronavirus 2 (SARS-CoV-2). It has spread worldwide leading to an ongoing pandemic. This pandemic has ravaged the world on an unprecedented scale. By April 2021, 141 million people have been infected and there are over 3 million deaths [10]. Chest X-Ray (CXR) is one of the important, non-invasive clinical diagnosis tools that helps to detect COVID-19 and other pneumonia for affected patients.

Using deep learning for X-ray classification is an ongoing research area and recently there have been promising models proposed for COVID-19 classification. The problem that all of these models face is an imbalanced dataset due to the limited number of COVID CXR images available.

FLANNEL is a COVID-19 CXR classification model proposed by Zhi Qiao et al. [7] that has been shown to accurately detect COVID-19 even when trained with only 100 available COVID-19 x-ray images. There are two core components for the FLANNEL architecture, the first is that it uses an ensemble [3] of five independent base models that predict the classification of the CXR. Each of the predictions are then passed through another neural weight network to determine the final prediction classification. The goal of the ensemble is to increase the robustness and accuracy of the network since each base model should capture patterns in the images independently [8]. The second core component for the FLANNEL is its use of the special Focal Loss [5] function, a modification of the standard cross-entropy loss that places a focus on the imbalance negatives by applying down-weights to well-classified examples. Focal Loss has been known to improve performance for imbalanced datasets.

Park et. al [6] has also created a deep learning model that has been proven to be effective on detecting COVID-19 when trained with limited datasets. The approach taken was to first detect lung contours of the CXR and perform segmentation. The motivation for performing segmentation first is that the patch based model focuses on the lung area since it's the primary region of interest used to perform analysis. In general, standard biomarkers [6] from CXR images analyzed are the following

1. Lung Morphology

2. Mean Lung Intensity

3. Standard Deviation of Lung Intensity

4. Cardiothoracic Ratio (CTR)

Thus it could be observed that most of the initial diagnosis is carried out from CXR images by concentrating on the lung area. We also find this strategy also makes the model less susceptible to noise happening outside the lung region. After the lungs have been segmented, patch-based classification is performed. Patch-based classification involves selecting random crops or patches across the image for a set number of times and then performing classification on each patch. Afterwards, the final prediction of the image is made by majority voting based on the prediction of each patch. Conclusion provided in the patch based paper [6] by Park and Ye, it is clear that the patch-based classification outperformed the models that used the whole image for a limited train set data. As we have an imbalanced dataset with limited COVID 19 CXR images, we are optimistic that utilizing patch-based classification models for the FLANNEL ensemble with the combination of focal loss optimization would result in a performance improvement.

Our goal is to take the novel ideas of each approach listed above with the goal of improving performance. To accomplish this we will make modifications to the existing FLANNEL architecture by first pre-processing the CXR images by performing segmentation of the lung contours. Afterwards, we will then update the independent base models in the ensemble to be patch-based classifiers. We call this new architecture "Patched FLANNEL". The network structure is shown in Figure 1 and similar to FLANNEL consists of two stage approach.

1.1 Related Work

Here we discuss some of the related works that are being carried out in this area on using deep learning techniques to detect COVID-19. Most of these works either used CXR or CT scans for patients to detect COVID-19. Our current research also falls in the same lines to accurately classify the patients CXR images to COVID-19 class or non COVID-19 classes.

1.1.1 AI-Covid

X. Bai and Wang [1] were able to create an AI system that could differentiate COVID-19 and other pneumonia using a chest CT scan. They approached this as a classification problem and used the EfficientNet B4 architecture which was a CNN based network. They were able to achieve results of 96% accuracy, 95% sensitivity, 96% specificity, and an area under receiver operating characteristic curve of 0.95 and an area under the precision recall curve of 0.90. When compared with radiologists on the same test dataset, the AI system performed better. This study concluded that the AI can support radiologists in detection of COVID-19 in Chest CT images.

1.1.2 COVID-Net

Wang L, Qiu Z, Wang A, et al. are able to create COVID-Net [9] architecture by considering COVIDx dataset which contains 13,975 CXR images for training and experiments.

COVID-Net architecture makes heavy use of a lightweight residual 'projection expansion projection extension' (PPEX) design pattern that contains multiple levels of convolution layers with fully connected layers and a softmax at the end. COVID-Net achieved higher test accuracy than other architectures such as VGG-19 and ResNet-50.

1.1.3 Focal loss for dense object detection

Lin T, Goyal P, Girshick R propose Focal loss [5], a modification to the standard cross entropy criterion that focuses weights for loss on hard examples versus well classified examples. This is accomplished by adding a factor $(1-p_t)^\gamma$ to the standard cross entropy criterion where setting $\gamma > 0$ reduces the relative loss for well-classified examples ($p_t > .5$). This results in achieving higher accuracy than using the standard cross entropy loss and surpassed speed and accuracy when compared with state of the art two stage detectors; Faster R CNN Variants.

1.1.4 Ensemble Models

FLANNEL model applies ensemble approach to combine multiple base learners to get classification from each model. As shown by Larse Kai Hansen and Peter Salamon [3] compared to individual model, a better classification can be achieved by training an ensemble of neural networks on same data and then using a consensus scheme to decide the collective classification by vote.

Modular ensemble models have also been shown to perform better and reduce training time in several researches [8]. It has been also shown to reduce model complexity and making the overall system easier to understand.

1.1.5 Noise-robust segmentation of COVID-19 from CT images

This is a CNN model [9] developed to be effective with detection of COVID-19 lesions from CT images that have a lot of noise. This paper discusses how Wang et al developed a novel noise-robust learning framework based on self-ensembling of CNNs. To better deal with the complex lesions, a novel COVID-19 Pneumonia Lesion segmentation network (COPLE-Net) was proposed that uses a combination of max-pooling and average pooling to reduce information loss during downsampling, and employs bridge layers to alleviate the semantic gap between features in the encoder and decoder. Experimental results with CT images of 558 COVID-19 patients showed the effectiveness of the noise-robust Dice loss function, COPLE-Net and adaptive self-ensembling in learning from noisy labels for COVID-19 pneumonia lesion segmentation. To make the training process robust against noisy labels, a novel noise-robust Dice loss function was proposed and integrated into a self-ensembling framework, where an adaptive teacher and an adaptive student are introduced to further improve the performance in dealing with noisy labels.

2. METHOD

The primary objective was to improve the detection of COVID-19 in CXR images with a multi-classifier model that can detect four categories: Normal, Pneumonia Viral, Pneumonia Bacteria and COVID-19. The baseline we will be comparing against is the original FLANNEL architecture. We used the same datasets that were used in the FLANNEL paper, the
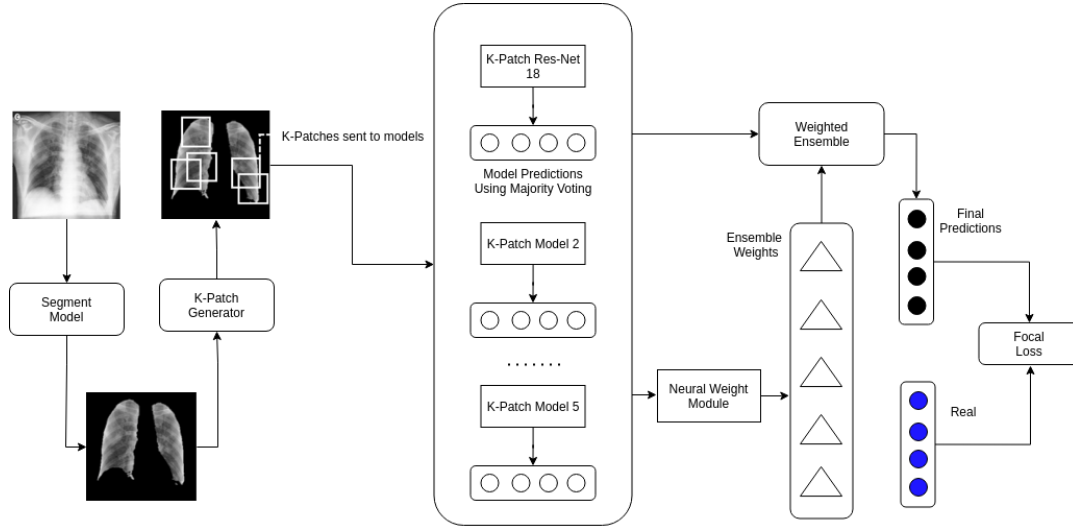
Figure 1: FLANNEL Improvement

COVID Chest X-ray Dataset [2] from GitHub and the Kaggle Chest X-ray images dataset. Similar to the FLANNEL paper, we also restricted the types of images used to anteroposterior (AP) or posteroanterior (PA). The restricted images were then labelled appropriately into one of the four categories.

2.1 Segmentation Training

The first major data pre-processing step that we performed on our dataset was segmentation. In order to accomplish this, we recreated the same segmentation network that Park et al. used for their patch-based classification; FC-DenseNet103 [4]. We trained the FC-DenseNet103 model using PyTorch to produce a mask of the lung contours of a CXR image. The datasets that were used to train the segmentation network were the Japanese Society of Radiological Technology (JSRT) dataset which contained 247 PA CXR images and the Segmentation in Chest Radiographs (SCR) database which contains segmentation masks for the CXR images from the JSRT dataset. The JSRT/SCR dataset were randomly split where 80% of images were used for training and 20% were used for validation; this resulted in 197 images being used for training and 50 images being used for validation for the JSRT dataset as shown in Table 1. Since CXR images from different data sources will come in a wide variety of formats, the JSRT dataset was pre-processed by performing data type casting to float32, histogram equalization to adjust the contrast, gamma correction to adjust brightness and standardizing the image size by resizing it to 256x256. During training, the network parameters were initialized with a random distribution and the Adam optimizer was used with an initial learning rate of 0.0001. The learning rate was decreased by a factor of 10 when there was no improvement in the loss. The Jaccard Index (JI) was used to evaluate the model during training since we were comparing the similarity of the mask produced by the network to the mask provided in the SCR dataset. An early stopping strategy was used based on the validation performance to prevent the model from overfitting.

We then applied the trained FC-DenseNet103 segmentation model on the AP and PA CXR images from the Covid Chest X-ray and Kaggle X-ray datasets. The original inference script provided by Park et. al would produce two outputs, a numpified version of the CXR and a numpified version of the mask separating the lung contours. The numpified version of the mask is just 0s and 1s where the 1s represent the area of the lung contours. We modified the inference script to apply the mask to the CXR by performing together by performing multiplication, we then saved the numpy compressed version of the masked CXR. This modification has two benefits, the first being that less disk space is used and the second being that our dataloader for the patch-based classifiers can improve performance since they no longer have to be responsible for applying the mask to the CXR as which was done by Park et. al. We then split the masked CXR dataset using a train-test ratio of 4:1 to randomly generate train test splits. To ensure reporting accurate performance on the base models, we used five fold cross validation while training. The detailed statistics are shown in Table 2. 2.

2.2 Base model training

The next improvement that we produced was creating patch-based classifiers. Similar to the original global base models in FLANNEL, the patch base models used were pretrained from ImageNet[1] to account for the small size of the dataset. The pre-processed images were first resized to 1024x1024 to be as close to the original pixel distribution. The masks generated from the FC-DenseNet103 segmentation model were also upsampled to 1024x1024 to match the new CXR image size. The resized images were then masked with the lung-contours and passed as input to the patch-based classifier. The patch-based classifier then produced k number crops/patches of size 224x224 from the CXR. To limit patches outside the lung area, the random points were forced to be within the lungs and the random point was used as the center of the patch. During inference, the k should

---

[1]http://www.image-net.org/challenges/LSVRC/index

be large enough to ensure that the lung pixels are covered multiple times. Each patch is then fed into a network to produce a prediction. The confidence score was calculated for each category by calculating the percentage of predictions for each class based on the k patches. The optimization algorithm used during training was the Adam optimizer with a learning rate of 0.00001. An early stopping strategy based on validation performance was applied and a weight decay and L1 regularization were used to prevent overfitting. The best model is selected among 200 epochs training.

2.3 Ensemble model learning

Ensemble model learning step is similar to baseline FLANNEL paper. We take N base models predictions and concatenate them as f and feed them in neural weight module to learn base model weight.

We calculate outer product ff^t which is flattened and fed into dense neural network with TanH layer to map features into base models weights. Then we train the ensemble model to learn optimal weight combination by feeding linear combination of predictions and weights of base models. The neural weight module uses a modified Focal loss function to handle multiclass classification.

The neural weight module uses a modified Focal loss function to handle multiclass classification. It downweighs the well classified classes, in-favor of poorly classified classes so the model can focus on learning imbalanced examples.

$$LossFunc = FocalLoss(\hat{y}, y) \tag{1}$$

$$= \sum_{m=1}^{M} -\alpha_m y_m (1 - \hat{y}_m)^\gamma \log \hat{y}_m \tag{2}$$

Where $(1 - \hat{y}_m)^\gamma$ is a modulating factor with tunable focusing parameters γ and α_m [7]. α_m is set to be inverse class frequency of each class.

The overall algorithm is shown in Algorithm 1.

Table 1: FCDenseNet103 Segmentation Training & Validation Dataset

Dataset	Number of images
Training	197
Validation	50

2.4 Considerations

Here are our considerations discussed below -

- The pretrained model for segmentation (FC-Densenet103) will perform well on the datasets used in FLANNEL [7] paper.

- The number of patches(K) to be 100 to start with, will be fine tuned after evaluating the results.

- The patch image size will be chosen as 224X224 initially and will be fine tuned after evaluating the results.

3. RESULTS

We chose 5 base models for FLANNEL framework, Densenet161, InceptionV3, Resnet152, ResneXt101 and Vgg19_bn. These

---

Algorithm 1: FLANNEL with patch-by-patch Training

Input :
X-ray Images, Class Labels
Segmentation Model
Base Models $\{Learner_1, Learner_2, \ldots, Learner_n\}$
(Define B as batch size)
(Define K patch count)
Stage 1:
Run segmentation network on the dataset to generate masks for each CXR image.
Stage 2:
For each *batch of images from input images and labels* **do**
1. Fetch the segmented mask and image.
2. Resize the CXR image to 1024x1024.
3. Upscale the mask to 1024x1024.
4. Separate image into random k patches.
5. Pass random k-patches to base models.
7. Get mean probability score from all Base Models.
$P_i = Learner_i(X) \in R^{B \times 4}$, where i = 1,...n
8. Get Learner weights.
$W = NeuralWeightModule([P_i, i = 1, .., n]) \in R^{B \times 5}$
9. Linear Combination for Prediction
$\hat{Y} = Softmax(\sum_{i=1}^{n} W_i P_i) \in R^{B \times 4}$ (where W_i represents i-th column of W)
10. Loss $= FocalLoss(\hat{Y}, Y)$
11. Back-propagate on Loss and update parameters
End

---

models were fine-tuned using default parameter values, settings and by using the Adam optimizer. We compared FLANNEL with these 5 base models of the framework.

The FC-DenseNet103 segmentation model was implemented in PyTorch and trained on a NVIDIA 1080 GPU. The operating system was windows 10 pro and python 3.8 was used. We are planning to create and train patch-based versions of the base models that will use the masked version of the same images from the dataset. We will then re-run the FLANNEL with the patch-based models and compare performance. In addition to the improvements, we are also planning to compare 2 recent COVID-19 deep learning models, COVID-Net [9] and AI-COVID [1].

3.1 Evaluation strategy

Our main goal is to study the detection of COVID-19 among different respiratory x-ray images. We first measured the overall accuracy and precision of all 4 classes of x-ray images (COVID-19 viral pneumonia, non-COVID-19 viral pneumonia, bacterial pneumonia and normal images).

For each class of image, we record precision and recall values for each fold. We calculate F1-score for each fold and then average them to calculate the mean F1 score.

We are evaluating the global base models independently, the global ensemble, the patch-based models independently and the patch-based ensemble.

Table 2: Experimental data description

Source		Total	COVID-19	Viral	Bacterial	Normal
Old data	CCX data	119	100	11	7	1
	KCX data	5389	0	1492	2780	1117
Current data	CCX data	554	478	16	42	18
	KCX data	5856	0	1493	2780	1583
View Distribution	AP view	6163	282	1501	2789	1591
	PA view	247	196	8	33	10
Training/test splits	Training	5127	378	1509	2291	1288
	Testing	1283	100	339	531	313
	Total	6410	478	1509	2822	1601

AP: anteroposterior; CCX: COVID Chest X-ray; COVID-19: coronavirus disease 2019; KCX: Kaggle Chest X-ray; PA: posteroanterior.

Table 3: Performance comparison on F1 score: Class-specific F1 score is calculated using 1 class vs the rest strategy

	COVID-19	Pneumonia virus	Pneumonia bacteria	Normal	Macro-F1
Original FLANNEL					
Densenet161	0.7694 (0.03)	0.5901 (0.05)	0.8030 (0.01)	0.8875 (0.02)	0.7625 (0.02)
InceptionV3	0.8938 (0.01)	0.6413 (0.03)	0.8112 (0.02)	0.9015 (0.03)	0.8120 (0.02)
Resnet152	0.8302 (0.02)	0.6218 (0.02)	0.8046 (0.01)	0.9080 (0.00)	0.7911 (0.01)
ResNeXt101	0.8197 (0.03)	0.6151 (0.04)	0.8016 (0.01)	0.9046 (0.01)	0.7852 (0.02)
Vgg19_bn	0.8753 (0.02)	0.6023 (0.01)	0.8016 (0.01)	0.8950 (0.00)	0.7936 (0.00)
FLANNEL	0.9239 (0.01)	0.6675 (0.02)	0.8306 (0.01)	0.9322 (0.00)	0.8385 (0.01)
Patched FLANNEL					
Densenet161	0.8994 (0.02)	0.5815 (0.02)	0.8171 (0.01)	0.9195 (0.01)	0.8043 (0.01)
InceptionV3	0.8974 (0.03)	0.6161 (0.00)	0.8286 (0.00)	0.9351 (0.01)	0.8193 (0.01)
Resnet152	0.8738 (0.02)	0.5527 (0.03)	0.8204 (0.00)	0.9133 (0.00)	0.7901 (0.01)
ResNeXt101	0.8978 (0.01)	0.5875 (0.01)	0.8215 (0.01)	0.9200 (0.01)	0.8067 (0.00)
Vgg19_bn	0.8870 (0.03)	0.5786 (0.03)	0.8201 (0.00)	0.9159 (0.01)	0.8004 (0.01)
FLANNEL	0.9121 (0.02)	0.6009 (0.01)	0.8270 (0.01)	0.9319 (0.01)	0.8180 (0.01)
FLANNEL_OldData	0.8168 (0.03)	0.6063 (0.02)	0.8267 (0.00)	0.9144 (0.01)	0.7910 (0.01)

The values in parentheses are the standard deviations.

3.2 Implementation Details

The FC-DenseNet103 segmentation model was implemented in PyTorch and trained on a NVIDIA 1080 GPU. The operating system was windows 10 pro and python 3.8 was used. FLANNEL with patch-based classification are implemented in PyTorch and are trained on 4 different Amazon Web Services Elastic Compute Cloud virtual machines each featuring a single NVIDIA Tesla V100 GPU. The base models are fine tuned using pre-trained models. The data are augmented with random flips, crops and scaling during the fine tuning process.

We created and trained patch-based versions in the same environment as the original FLANNEL base learners. The primary difference was that the dataset fed to the patch-based learners was the masked CXR images. Since the CXR images were already masked, no random flips, crops or scaling was applied to the data for training.

After the base models are trained, FLANNEL is trained by passing in the concatenated output layers of the base models as the input features.

3.3 Experimental Results

3.3.1 Segmentation Training

Training the Segmentation Network on the JSRT/SCR dataset had a Jaccard Index (JI) score of 93.39% for creating the lung contour masks. The figure 2 shows the mask creation and applying the mask on the image.

Figure 2: Segmentation Training

3.3.2 FLANNEL

We compared original FLANNEL base models and ensemble performance with the patched FLANNEL. Because COVID-19 class is heavily imbalanced compared to other categories, overall accuracy would not be the appropriate measure for performance evaluation. Overall accuracy wouldn't be able to show performance increase in COVID-19 detection, instead we use F1-score for COVID-19 vs rest comparing the different models. As shown in figure **??** We can see the ensemble approach in the original FLANNEL clearly outperforms state-of-the-art base models in detecting COVID-19. We however, don't see the same performance gain in the

patched FLANNEL approach where ensemble performance is slightly worse than the base models. We do notice an improvement in patched base models compared to the original base models. We also compare original FLANNEL and the patched FLANNEL ensemble performance with FLANNEL run as done in the research paper and clearly see improvement. This improvement can be contributed to having improved COVID-19 distribution compared to the original dataset containing only 100 images [7].

We also compare the patched and original FLANNEL performance via confusion matrix as shown in figure 4 and Fig 5. We see both patched and original FLANNEL performs similarly in detection of COVID-19 images where it has higher precision and recall than other two types of Pneumonia. Both models struggle with Pneumonia viral images classification and misclassifies them as Pneumonia bacteria images.
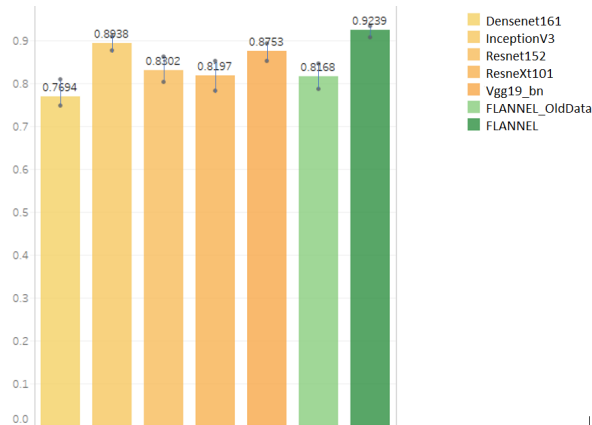
In this section, We compared FLANNEL ensemble performance with the independent performance for each of the base models. Due to imbalance dataset, overall accuracy is not the appropriate measure for evaluation of the model. With this imbalance, even a significant increase in COVID-19 detection performance will not affect overall accuracy much. So, we will use F1 score for COVID-19 vs the rest comparing different models. As shown in the figure 3, clearly FLANNEL outperformed the other state-of-the-art models in detecting COVID-19 cases.

In Table 3, we also show F1-score for each classification and macro F1-score for all classes. In Table 3, we can see FLANNEL performed better than base models. We also see with improved data FLANNEL scores are better than when run with old dataset containing only 100 COVID-19 images [7]. We also compared the performance of the original FLANNEL ensemble with the patched ensemble using micro-F1 score and saw a slight increase in overall performance compared to the original approach.

We also compare the patched and original FLANNEL performance via confusion matrix as shown in Figure 8 and Figure 9. We see both patched and original FLANNEL performs similarly in detection of COVID-19 images where it has higher precision and recall than other two types of Pneumonia. Both models struggle with Pneumonia viral images classification and misclassifies them as Pneumonia bacteria images.

We also present the ROC curve in Figure 4 and PR curve in Figure 5 to show diagnostic ability of patched FLANNEL. As ROC curve can be misleading for highly imbalanced classifications, we also present Precision-Recall curve for patched FLANNEL. As we can see ROC curve AUC all models are performing well they have very less false positives. However when we look at PR curve, we could see all models performance differ and InceptionV3 and Ensemble model performing better than others.
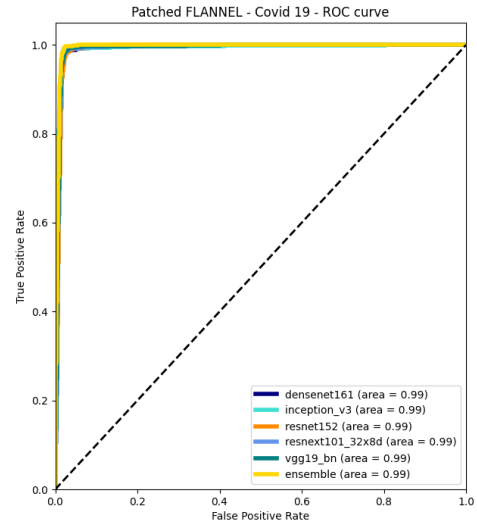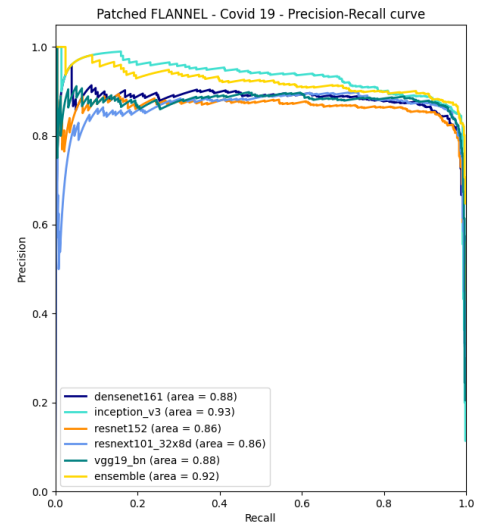

Figure 4: Patched FLANNEL ROC Curve

Figure 5: Patched FLANNEL PR Curve

We also provided the visual description of FLANNEL performance, via confusion matrix as shown in figure **??**. As

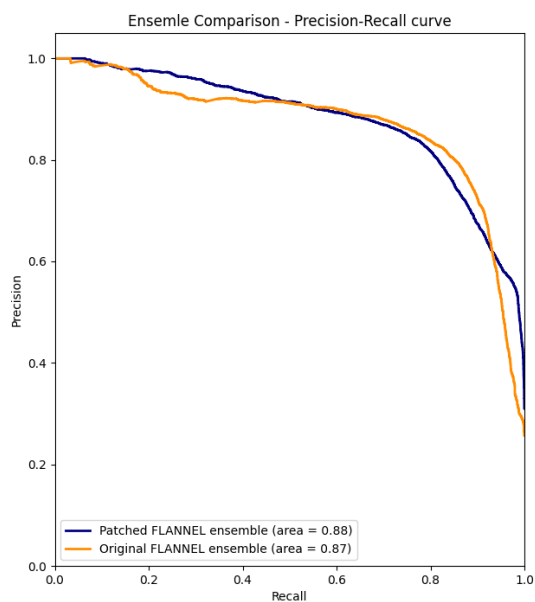Figure 3: FLANNEL Improvement

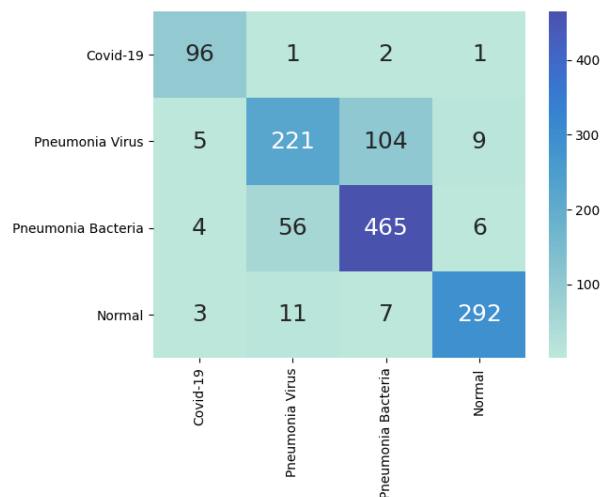Figure 6: Ensemble Comparision PR Curve

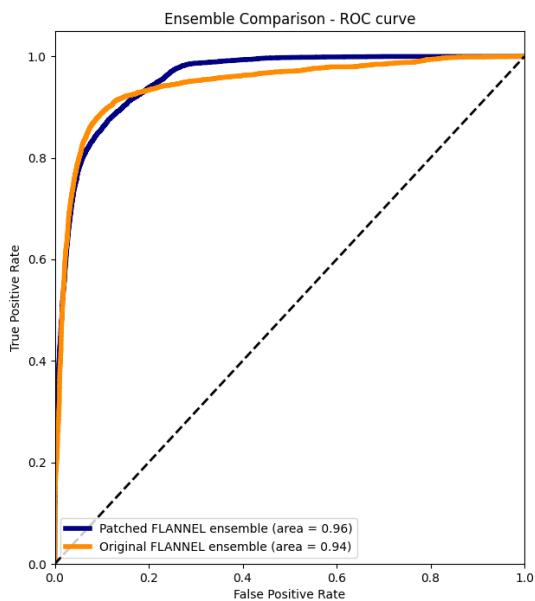Figure 8: Original FLANNEL Confusion Matrix

Figure 7: EnsembLe Comparision ROC Cuve

Figure 9: Patched FLANNEL Confusion Matrix

the matrix depicts, For COVID-19 identification, FLAN-NEL has higher precision and recall than the other 2 types of pneumonia. This proves FLANNEL can distinguish pneumonia images from normal images and differentiate chest x-ray images of COVID-19 against other pneumonia images.

4. DISCUSSION

Training the original FLANNEL model was extremely slow already where training a single model takes on average 6 hours. When using the original architecture for the patch-based models, their training process was even slower due to two reasons. The first is that the patch-base model dataloader was originally responsible for applying the mask to the cxr image, this was addressed by transitioning the responsibility to the segmentation task to immediately apply the mask to the CXR. The second reason for the patch-based models being slow is that a classification is run for each patch sequentially. This increases the complexity from N to kN where k is the number of patches. We were unable to address this due to time constraints but we believe parallelizing the patch predictions could lead to major improvements.

After training the patch-based models we were hoping to see substantial improvements similar to Park et al. but we only noticed minor changes in performance where some models slightly increased while others decreased. Two models that had an increase in average precision performance were inceptionv3 and densenet161. While resnet152, resnext101 and vgg19 had minor decreases in average precision. Even though three of the base-models had decreased performance, the patched ensemble still had a minor improvement over the base ensemble in average precision by 0.01. We were originally hopeful to have more significant increases in performance. Some of the reasons that could explain this result is the segmentation that generated the masked CXR is inaccurate and is masking important information surrounding the edges of the lungs. This hypothesis will need to be verified by a medical expert. Another reason the patch-based method was not as effective was that local patterns within the lung areas of a CXR are less important than the global patterns detected within a lung. This hypothesis can potentially be tested by increasing the patch size and measuring performance again.

Running FLANNEL with improved data distribution We realized very early in the project that running FLANNEL model using five base models and 200 epochs for five foldes is going to take at least 3-4 days on a Tesla V100 GPU or equivalent. We had to find a solution on both cost and runtime in order to have results early. We tried multiple optimization methods such as increasing the number of workers, mounting training images in memory to bring the runtime down. We also used spot instances in parallel to bring the cost down. We were able to complete training and evaluation of the FLANNEL model in 36 hours and considerably less cost around 100 dollars.

We could have done below things to improve the patch classifier performance. We removed the weight assignment step from the patch classifier, because we thought the classification output is already being passed through an ensemble method where a neural network learns proper weight. We could have also run it for 200 epochs like FLANNEL and implemented learning rate adjustment at 150 epochs.

5. CONCLUSION

We had two major goals for this project. To faithfully reproduce FLANNEL on an updated dataset with improved distribution of COVID-19 images and to apply segmentation and patched classification to improve the COVID-19 detection performance of FLANNEL model.

We ran the base models and FLANNEL ensemble on the new dataset using all five folds and 200 epochs. With the improved distribution of COVID-19 data we see FLANNEL outperforms the metrics as seen in the Original FLANNEL paper by 13This large increase in performance highlights the importance of curating a rich dataset.

Then we created the Segmentation model that produced masked CXR images that displayed only the lung contours. These masked images were then used as a dataset for patch-based versions of the FLANNEL model. The performance of the patch-based models was very similar to their "global" counterparts with three of the five models having a slight increase in performance while the other two had a slight decrease. We then ran the ensemble on the outputs of the patch-based classifier and did not note major improvement in classification performance. For COVID-19, ensemble on patched classifiers performed slightly worse than Original FLANNEL ensemble. However, for overall classification the average precision increased by 0.01 over the Original FLANNEL.

We were able to complete patch classifier run earlier than Original FLANNEL (stage-1 and stage-2) where early stopping and less epochs (100 vs 200 epochs for Original FLANNEL).

We were partially able to achieve our goal of improving the original FLANNEL architecture using patch-based models. Even though the performance was slightly increased, we see both Original FLANNEL and Patched FLANNEL clearly outperforms the other base models.

6. CONTRIBUTION

All authors were actively involved in Patched FLANNEL development and implementations. Major contribution from authors are

Maneesh: AWS Setup, batch run of FLANNEL and patch-based models on AWS, Development of patch-based classification and ensemble, project report, GitHub documentation Satish: FLANNEL checkpoints, output graphs and reports development, Github documentation Raman: segmentation, patch-based classification development, output graphs and reports development, project report, GitHub documentation Srikanth: segmentation, patch-based classification development, project report,GitHub documentation

7. ACKNOWLEDGEMENT

8. APPENDIX

GitHub source code for the Patched FLANNEL `https://github.com/mannbiher/DeepLearningForHealthCareProject`

9. REFERENCES

[1] H. X. Bai, R. Wang, Z. Xiong, B. Hsieh, K. Chang, K. Halsey, T. M. L. Tran, J. W. Choi, D. C. Wang, L. B. Shi, J. Mei, X. L. Jiang, I. Pan, Q. H. Zeng, P. F. Hu, Y. H. Li, F. X. Fu, R. Y. Huang, R. Sebro, Q. Z. Yu, M. K. Atalay, and W. H. Liao. Artificial Intelligence Augmentation of Radiologist Performance in Distinguishing COVID-19 from Pneumonia of Other Origin at Chest CT. *Radiology*, 296(3):E156–E165, 09 2020.

[2] J. P. Cohen, P. Morrison, L. Dao, K. Roth, T. Q. Duong, and M. Ghassemi. Covid-19 image data collection: Prospective predictions are the future. *arXiv 2006.11988*, 2020.

[3] L. K. Hansen and P. Salamon. Neural network ensembles. *IEEE Transactions on Pattern Analysis and Machine Intelligence*, 12(10):993–1001, 1990.

[4] S. Jégou, M. Drozdzal, D. Vázquez, A. Romero, and Y. Bengio. The one hundred layers tiramisu: Fully convolutional densenets for semantic segmentation. *CoRR*, abs/1611.09326, 2016.

[5] T.-Y. Lin, P. Goyal, R. Girshick, K. He, and P. Dollár. Focal loss for dense object detection, 2018.

[6] Y. Oh, S. Park, and J. C. Ye. Deep Learning COVID-19 Features on CXR Using Limited Training Data Sets. *IEEE Trans Med Imaging*, 39(8):2688–2700, 08 2020.

[7] Z. Qiao, A. Bae, L. M. Glass, C. Xiao, and J. Sun. FLANNEL (Focal Loss bAsed Neural Network EnsembLe) for COVID-19 detection. *Journal of the American Medical Informatics Association*, 28(3):444–452, 10 2020.

[8] A. Sharkey. On combining artificial neural nets. *Connect. Sci.*, 8:299–314, 12 1996.

[9] L. Wang and A. Wong. Covid-net: A tailored deep convolutional neural network design for detection of covid-19 cases from chest x-ray images, 2020.

[10] WHO Emergency Response Team. Weekly epidemiological update on covid-19 - 20 april 2021. Technical report, WHO, April 2021.